RC 22562 (W0209-063) September 16, 2002
Electrical Engineering

IBM Research Report

MARS2: An Advanced Femtosecond Laser Mask Repair Tool

Alfred Wagner, Richard Haight, Peter Longo
IBM Research Division
Thomas J. Watson Research Center
P.O. Box 218
Yorktown Heights, NY 10598

Research Division
Almaden - Austin - Beijing - Haifa - India - T. J. Watson - Tokyo - Zurich

MARS2: An Advanced Femtosecond Laser Mask Repair Tool

Alfred Wagner, Richard Haight, Peter Longo
IBM Semiconductor Research and Development Center (SRDC)
Research Division
TJ Watson Research Center
Yorktown Heights, NY 10598

ABSTRACT

Femtosecond pulsed lasers offer fundamental advantages over other techniques for repairing lithographic masks. Since the femtosecond ablation process is non-thermal, the spatial resolution is not degraded by thermal diffusion and is therefore limited only by optical diffraction. In addition, metal splatter, gallium staining, reduced optical transmission, beam induced charging, quartz damage, and phase errors inherent in other repair methods are eliminated.

A second generation femtosecond laser repair tool is described. The tool utilizes DUV optics which allow ~100nm mask features to be imaged. The laser beam is focused to a round, gaussian spot. This gaussian spot is scanned over the defect, thus allowing arbitrarily shaped repairs to be performed with a spatial resolution of ~100nm. Since the mask is not degraded in any way during the repair process, repairs can be performed iteratively by ablating small slices of the defect. Mask features can be trimmed to an RMS precision of ~5nm. The system is also highly automated: masks are loaded into the tool from a SMIF pod via a robot and the tool is controlled from a single screen operator interface. This new tool has been operating successfully in the IBM Burlington mask house since late 2001, and is currently IBM's primary repair tool for 248 and 193nm chrome on glass and phase shift masks.

INTRODUCTION

Over the past 5 years, the aerial image performance of wafer printing tools has not kept pace with the desires of the semiconductor industry. Numerous resolution enhancement techniques (RET) have been adopted to improve the aerial image. Most of these techniques involve modifications to the photomask, such as optical proximity correction, sub-resolution assist features, weak and strong phase shifting, and more stringent dimensional control. These mask RET's dramatically increase the complexity and cost of the photomask. They also make the mask far more susceptible to defects. Subtle variations in the optical transmission or phase over 100nm scale distances on the photomask are now likely to cause wafer defects. As a result, direct fabrication of an advanced photomask containing no defects is nearly impossible. Mask makers generally fabricate nearly perfect masks, locate the defects using automated inspection tools, and then remove these defects using mask repair tools. Since the optical quality of the repairs must also meet the stringent requirements placed on of the rest of the mask, the demands on repair tools have increased significantly.

Unfortunately, commercially available repair technologies utilizing focused ion beams[1-4] or nano/picosecond pulsed lasers [5,6] have not kept pace with the increased requirements. In the case of nano/picosecond pulsed lasers, excess absorber defects are removed via thermal ablation. The laser pulse heats the absorber, causing it to melt and explosively evaporate. The process splatters molten material in surrounding regions reducing the optical transmission and often producing new defects. In addition, the quartz substrate is partially ablated resulting in a phase error[7]. Finally, the spatial resolution is limited by thermal diffusion to ~500nm. While focused ion beams offer excellent spatial resolution, the ion beam interacts equally strongly with the absorber and the substrate. As a result, the optical quality of the repair is markedly degraded due to gallium implantation, radiation damage to the quartz, and the inevitable sputter erosion of the quartz in the repair region[8,9]. Furthermore, inadequate charge neutralization in FIB systems often causes imaging artifacts and large repair placement errors. Finally, FIB tools require frequent, time consuming setup and calibration, and the small beam currents needed to attain high spatial resolution result in very slow repair rates.

Femtosecond laser ablation offers fundamental advantages for mask repair [10,11]. When the duration of a laser pulse is less than a few picoseconds, material can be ablated from a substrate via a non-thermal process[12-14]. The light pulse directly excites a large fraction of the valence electrons to antibonding states, causing the material to enter the vapor phase before the electrons transfer their energy to phonons (heat). Since thermal effects are absent, the spatial resolution is determined by the size of the laser spot rather than thermal diffusion lengths. Furthermore, the optical quality of the ablated region on a photomask shows virtually no degradation in the optical transmission or phase. By coupling a femtosecond laser with an advanced tool architecture, we have been able to achieve a spatial resolution normally associated with FIB tools combined with the ease of use of laser based mask repair.

SCANNED GAUSSIAN FEMTOSECOND REPAIR TOOL

An advanced mask repair tool was developed at IBM which exploits the advantages of femtosecond laser ablation. The tool combines a femtosecond laser with deep ultraviolet (DUV) imaging optics, a precision air bearing stage, and a computer control system as shown schematically in Figure 1.

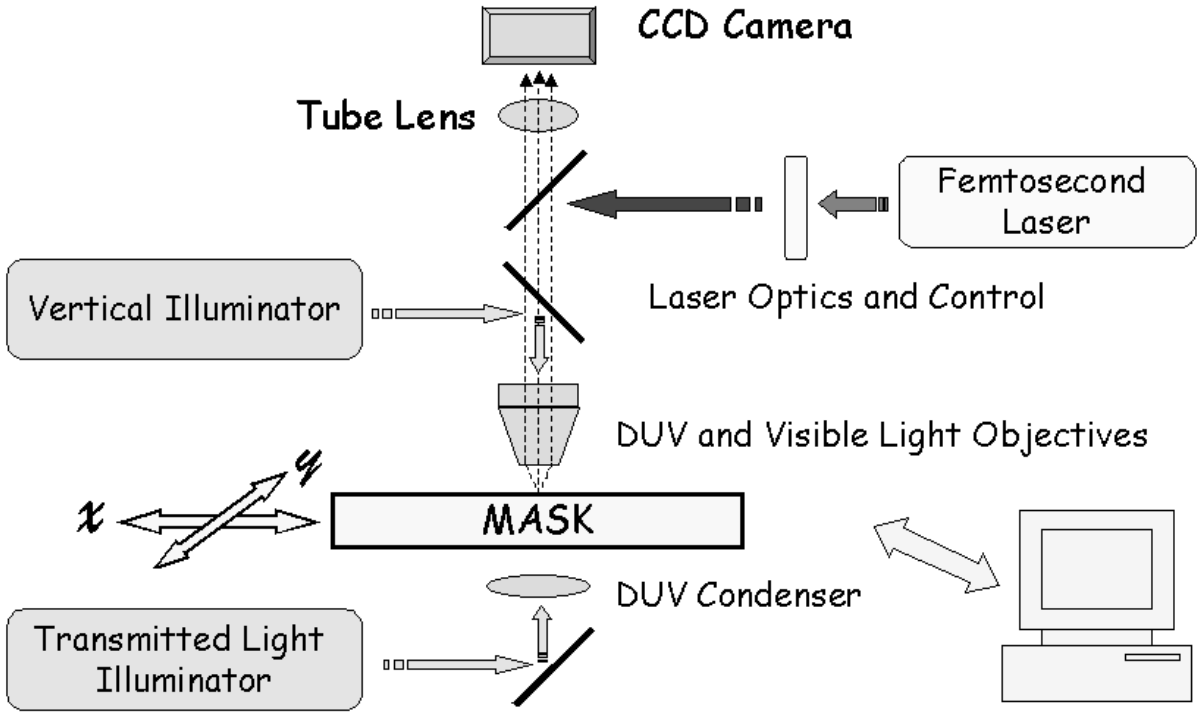

Figure 1: Schematic of IBM's scanned gaussian mask repair tool (MARS2) showing the femtosecond laser, stage, visible and DUV optical system, and control system.

The mask can be imaged in either transmitted or reflected light. Six objectives are available providing a wide range of magnification. Five of the objectives operate in the visible (approximately 400nm), while one objective operates in the DUV (248nm). The DUV objective provides images with a resolution on the order of 100nm and a field of view 28 by 22 microns. The DUV image can also be digitally zoomed by 2X to 16X to provide additional increased magnification. The DUV objective is also used for ablating defects. The tool incorporates an auto focusing system which keeps the

mask image and the laser beam in focus at all times. The laser produces pulses of light ~100 femtoseconds in duration at a 1 kHz repetition rate. The output beam from the laser is frequency tripled into the DUV, coupled into the DUV objective via additional optics and a beamsplitter, and focused onto the mask. We estimate that the laser spot on the mask has an approximately gaussian shape with a diffraction limited diameter of ~150nm. The intensity of the laser beam delivered to the mask is monitored and controlled via the computer to maintain the desired ablation set point. In addition, the beam is blanked using an electronic shutter which is under computer and hardware control. By scanning the mask relative to the focused laser spot and blanking the laser beam at appropriate times, arbitrarily shaped regions on the mask can be ablated.

The procedure for repairing a photomask is simple, rapid, and highly intuitive. The operator transports the photomask to the tool in a SMIF pod and places it on the loading station. All tool functions are controlled via the single operator control screen shown in Figure 2.

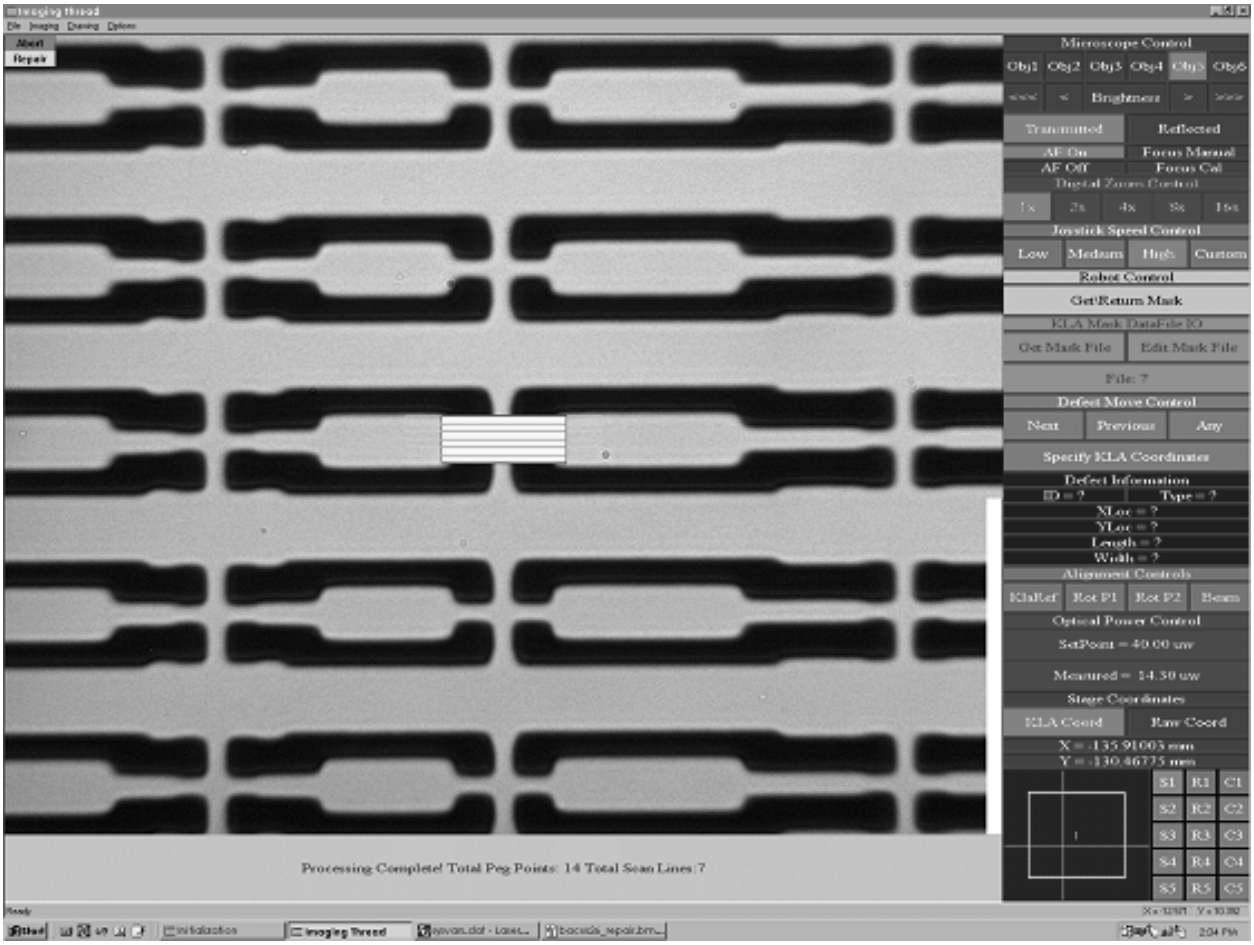

Figure 2: Operator Control Screen. All tool function such as magnification, imaging mode, inspection file transfers, mask loading, etc. are controlled via the menu boxes on the right hand side of the screen. Most of the screen contains a high resolution image of the mask. A DUV transmitted light image of an attenuated PSM mask is shown above. The field of view is 28x22 um, and the smallest steps in the mask features are approximately 400nm. The gray rectangular box in the center of the image represents the region that will be ablated by the femtosecond scanned laser beam.

The appropriate defect inspection file (e.g. KLA file) is transferred to the repair tool, and the load sequence is initiated. A robot then loads the mask directly into the tool from the SMIF pod. During the load process, the robot precisely orients the mask and places it on the stage with an absolute position accuracy of ~25 um and a rotational accuracy of approximately +/-0.02 degrees. The mask is automatically moved to fiducial marks which are used to determine and compensate for the residual rotation of the mask with respect to the stage coordinate system (typically +/- 0.02 degrees). The mask then moves to the reference mark stored in the inspection file, and the operator selects the appropriate mask feature. Since the original placement of the mask on the stage by the robot is so precise, the fiducial marks and KLA reference mark always appear in the field of view available to the tool operator. This eliminates the often tedious and error prone "hunt and peck" process common in commercial repair tools. The operator can then sort defects according to particular inspection classifications. The tool moves the stage to the defects by a simple mouse click on the tool control screen. Since the reference and align procedure is also highly accurate and precise, the defects always appear almost perfectly centered in the field of view. As shown in Figure 3, defects typically appear in the center of the CRT image screen with a maximum position error less than +/- 0.8um. This small position error ensures that the repair tool operator will correctly identify and repair the defect, even for masks with complex RET patterns and small, subtle

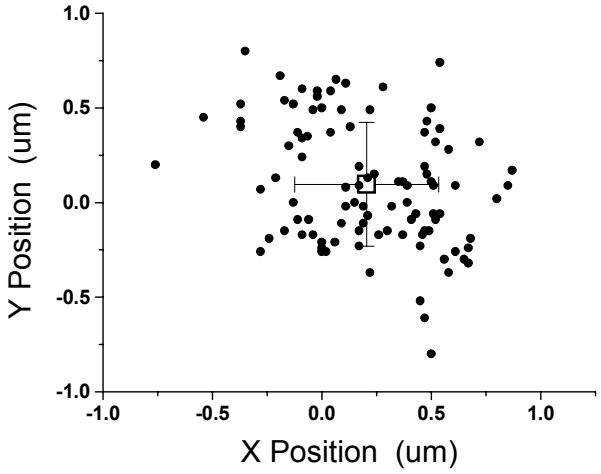

Figure 3: Position of 100 defects relative to the center of the CRT screen. The maximum error is +/-0.8um and the RMS error is ~0.3um.

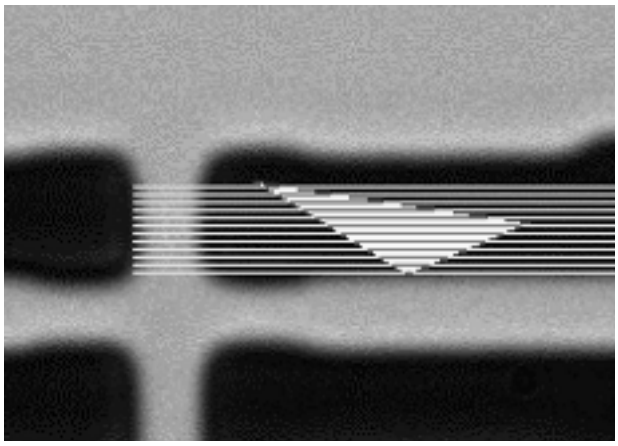

Figure 4: Portion of the DUV image in Fig 2 showing a triangular region to be ablated. Approximately 12 laser scan lines are indicated

defects. The operator then views the high resolution DUV image, identifies the defect, and manually outlines the region to be ablated. As shown in Figure 4, the triangular region in center of the image will be ablated. Several options are available for scanning the laser beam over the defect, including the scan direction, the spacing between scan lines, laser energy, etc. In addition, bias can be applied to the repair to adjust the final repair size to match the desired outcome. These parameters are typically set once for a particular mask material, and do not require any adjustment. After outlining the defect, the operator mouse clicks on the "Do Repair" button and the computer calculates the proper scanning sequence and initiates the repair. Typically, the entire process of outlining and ablating the defect and ablating takes a few minutes or less.

ADVANTAGES OF SCANNING A GAUSSIAN LASER BEAM

In previous laser based repair systems, a motorized rectangular aperture was illuminated by the laser beam, demagnified, and imaged onto the mask. These "imaged aperture" tools are thus limited to ablating rectangularly shaped regions. By scanning a small gaussian shaped femtosecond laser beam, our new tool overcomes this limitation and allows

polygonal features to be ablated. This is particularly useful for feature reconstruction; the rounded corners of the primary, OPC and assist features in an advanced photomask can now be accurately replicated. This is illustrated in Figure 5 which shows 6 "submarine" shaped features that were directly ablated into Cr using the scanned gaussian repair tool (MARS2). The rounded corners on the features accurately reflect the repair outline. In addition, the subtle variations in the size and/or shape of each feature were intentionally introduced by either i) making slight changes in the repair outline or ii) simply changing the bias that was applied to the repair outline. Imaged aperture laser repair tools are not able to produce the complex features shown in Figure 5a.

There is an additional advantage of scanning a gaussian shaped laser beam. Diffraction from the rectangular aperture in imaged aperture tools adversely effects the spatial distribution of light on the mask. Figures 5b and 5c shows ablations performed using an imaged aperture repair tool employing a femtosecond laser. Although the femtosecond laser

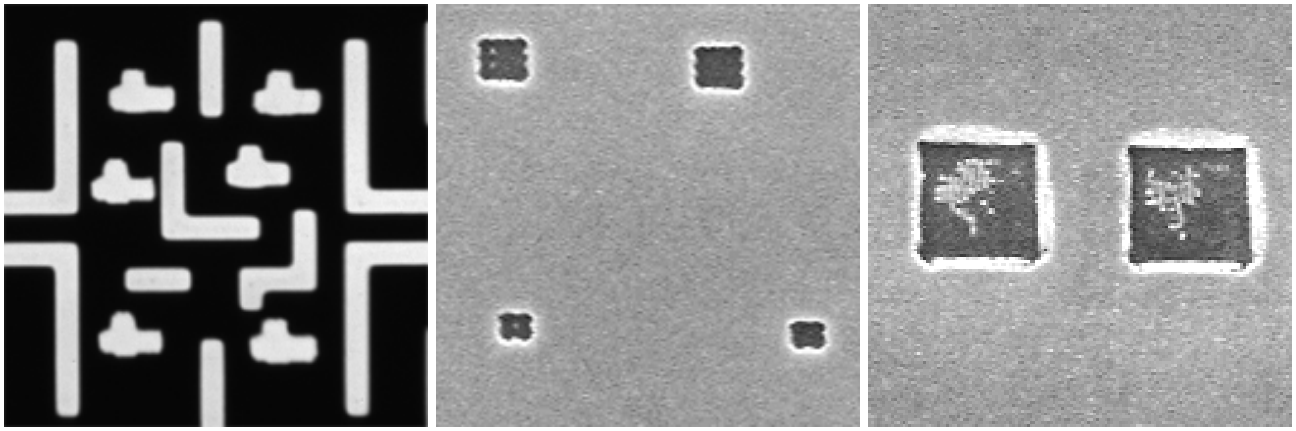

Figure 5: (a) By scanning the gaussian shaped femtosecond laser beam relative to the mask, complex feature such as the "submarines" shown in (a) can be ablated.. The subtle differences in the size and shape of the ablated "submarines" were intentionally produced. (b) Diffraction effects in an imaged aperture repair tool produce distorted ablated shapes. (c) Residual Cr dots and/or pits ablated into the quartz substrate can also result from diffraction in imaged aperture systems. These diffraction effects are eliminated in the new scanned gaussian repair tool (MARS2).

ablation process yields outstanding spatial resolution, the wiggles on the edges of the ablated rectangles (Fig 5b) and residual Cr dots (Fig 5c) are due to diffraction. Our new tool eliminates these diffraction artifacts and allows us to achieve the spatial resolution inherent in the femtosecond laser ablation process.

TOOL PERFORMANCE: IMAGING

A key feature of any mask repair technology is the spatial resolution of the imaging system. For advanced masks at the 90nm node, primary features on the mask are typically on the order of 360nm. However, the sub resolution features placed on the mask to enhance wafer print resolution (RETs) can be on the order of 1/2 to 1/4 the size of the primary feature. Thus the secondary features on the mask can be comparable in size to the images printed on the wafer. The imaging performance of the DUV optics incorporated in IBM's repair tool is illustrated in Figures 6 and 7. DUV transmitted light images of 150nm nominal contact holes in a Cr field, 150nm Cr contact dots, and 100nm equal Cr lines and spaces are shown in Figure 6. The images were zoomed digitally to increase the magnification and thus represent a small fraction of the field of view in the repair tool. In all cases (a-c), there is no enhancement of the image; only the image brightness is adjusted in the repair tool to give a pleasing image.

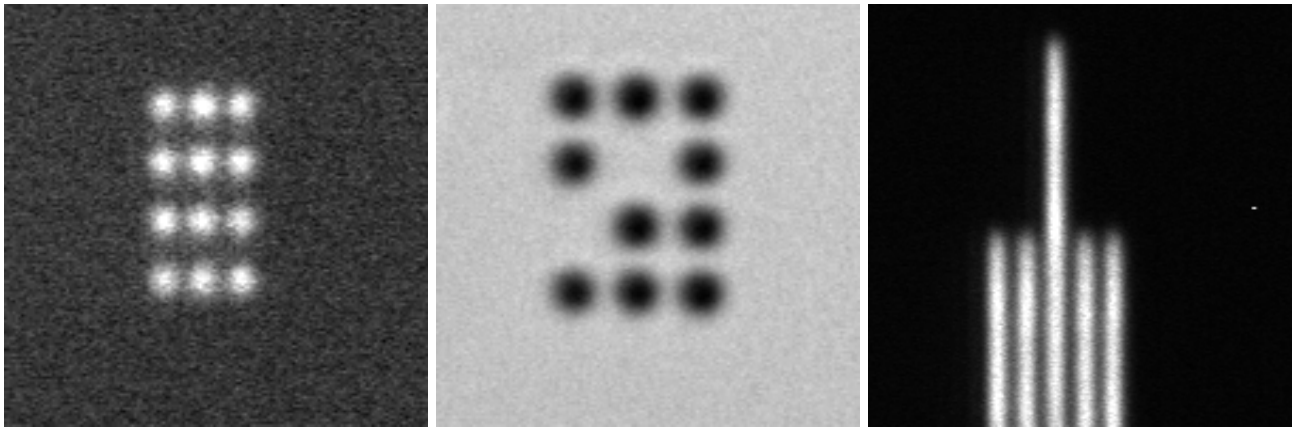

Figure 6: Transmitted light DUV images of nominal (a) 150nm holes in Cr on 300nm spacing; (b) 150nm Cr dots on 300 nm spacing, and (c) 100nm Cr lines and spaces. Two of the 12 Cr dots shown in (b) were removed with the MARS2 tool demonstrating ablation in tight geometries.

DUV images of a 193nm attenuated phase shift mask are shown in Figure 7. Again, the images were digitally zoomed in the tool to increase the magnification. The image in Figure 7a illustrates the complex OPC features present on state of the art masks. The image in Figure 7b shows clearly resolved 150nm assist features. Note that both COG and PSM masks produce high contrast, high brightness images with no artifacts. In addition, all PSM materials we have used image with nearly identical brightness and contrast. The images displayed in Figures 6 and 7 are representative of the real time (13 Hz) images obtained in the tool. Unlike FIB tools, no degradation in the mask occurs during imaging - there are no limitations on the length of time a site may be imaged.

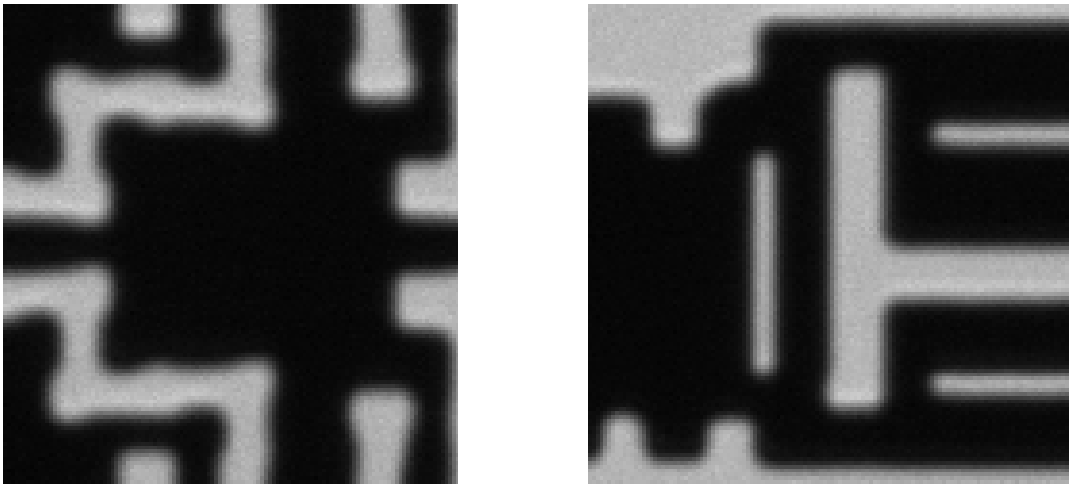

Figure 7: (a) DUV image of an 193nm attenuated PSM. The field of view is approximately 4.5x4.5 um, and the smallest OPC features are on the order of 100nm. (b) a PSM showing 150nm assist features (vertical and horizontal bars).

TOOL PERFORMANCE: ABLATION RESOLUTION AND REPAIR QUALITY

In addition to the high quality imaging shown in the previous section, an advanced mask repair tool must be able to remove material with high spatial resolution and accurate edge placement. Furthermore, the optical quality of the repairs must meet stringent requirements on transmission and phase error. The non-thermal ablation mechanism inherent in femtosecond laser processing, coupled with the advanced architecture of the MARS2 tool is uniquely able to meet all the requirements for advanced mask repair.

Figure 8 shows a simple demonstration repair. A triangular Cr defect intruding into a clear quartz region is shown near the center of Fig 8(a). Also shown in Fig 8(a) is a narrow horizontal quartz line below the defect, and a quartz triangle in the upper right. Both of these features were produced using the MARS2 repair tool to provide unique reference marks prior to the repair. The Cr defect was removed as shown in Fig 8(b) demonstrating an aligned repair. The displacement of the repaired horizontal edge relative to the existing features was less than 25nm, the optical transmission at 248nm was greater than 98% of the transmission in an unrepaired quartz regions, and the phase error due to quartz ablation was undetectable. Similar results are routinely achieved in manufacturing in the IBM Burlington mask house [15]. Unlike FIB tools, the MARS2 tool images using DUV light. Therefore, the optical quality of a repair can be determined using the MARS2 tool. Furthermore, the true optical displacement of a repaired edge can be measured with the repair tool. The ability to optically evaluate a repair within the MARS2 tool is a significant advantage over FIB repair.

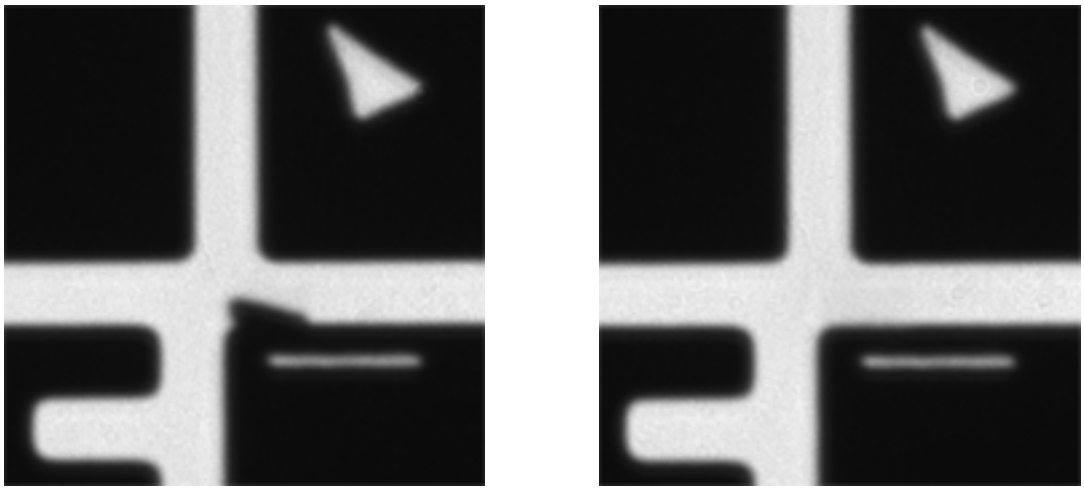

Figure 8: (a) Cr defect before repair. The defect is approximately 250nm high. The narrow horizontal quartz line below the defect and the quartz triangle were made with the MARS2 tool. (b) after repairing the defect. The repaired area is essentially perfect.

An even more fundamental advantage of the MARS2 tool is our ability to iteratively repair a defect. Regions on the mask can be repeatedly ablated with no degradation to the quartz substrate or mask absorber. Thus a defect can be repaired, and the optical properties and placement of the repair evaluated. If the optical transmission, placement accuracy, or feature fidelity is not within specification, the repair can be trimmed and reevaluated. This process can be repeated until the desired quality of repair is achieved. The precision of trimming an edge is demonstrated in a later section in the article entitled “Nibble Mode”. In general, repairs evaluated with the MARS2 tool correlate well with Aerial Image Measurements (AIMS).

Due to the non-thermal ablation mechanism, the MARS2 tool achieves outstanding spatial resolution. Figure 9 shows a DUV transmitted light optical micrograph and a scanning electron micrograph (SEM) of an ablated line. The line is approximately 160nm high, about equal to the diameter of the focused laser spot. Achieving linewidths that are comparable to the beam diameter is easy; careful control of the tool parameters is not necessary.

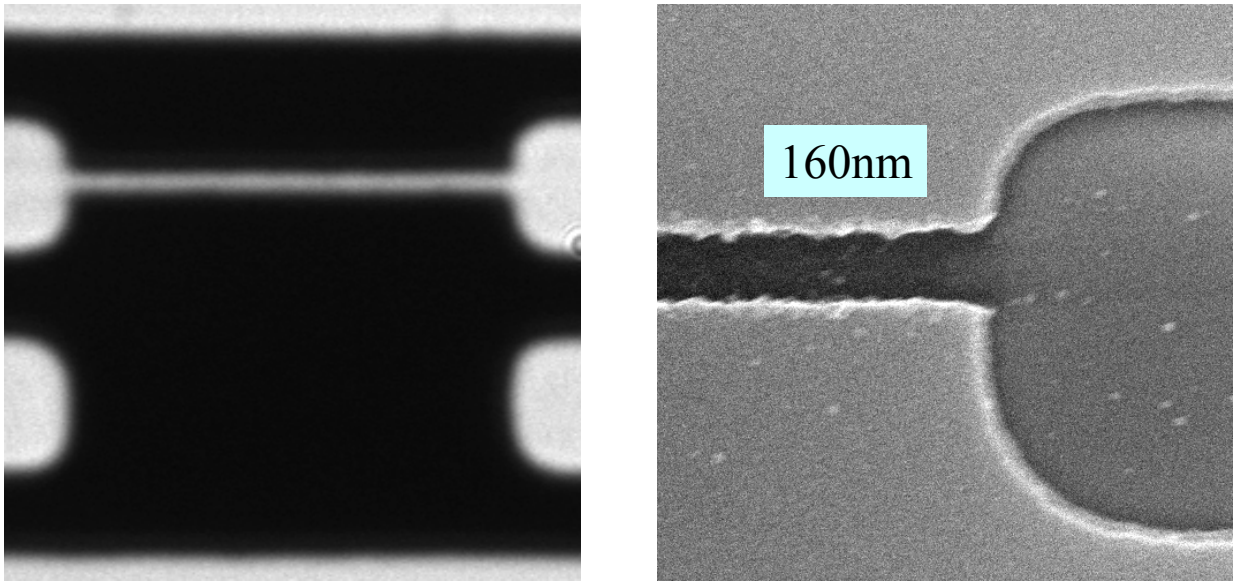

Figure 9: (a) DUV optical micrograph showing an line ablated using the MARS2 tool. (b) an SEM micrograph of the same feature shown in (a). The ablated line is ~160nm high.

However, the non-linearity of the femtosecond laser ablation process can be exploited to further enhance the ablation resolution. If the focus and the laser energy are carefully controlled, features which are substantially smaller than the diffraction limited gaussian beam diameter can be ablated. SEM micrographs of an ablated line and a dot which are approximately 1/2 the diameter of the focused laser spot are shown in Figure 10. The laser energy was increased until the ablated line and dot just began to transmit DUV light. The MARS2 imaging system was more than adequate for detecting the point at which the Cr was fully ablated down to the quartz substrate.

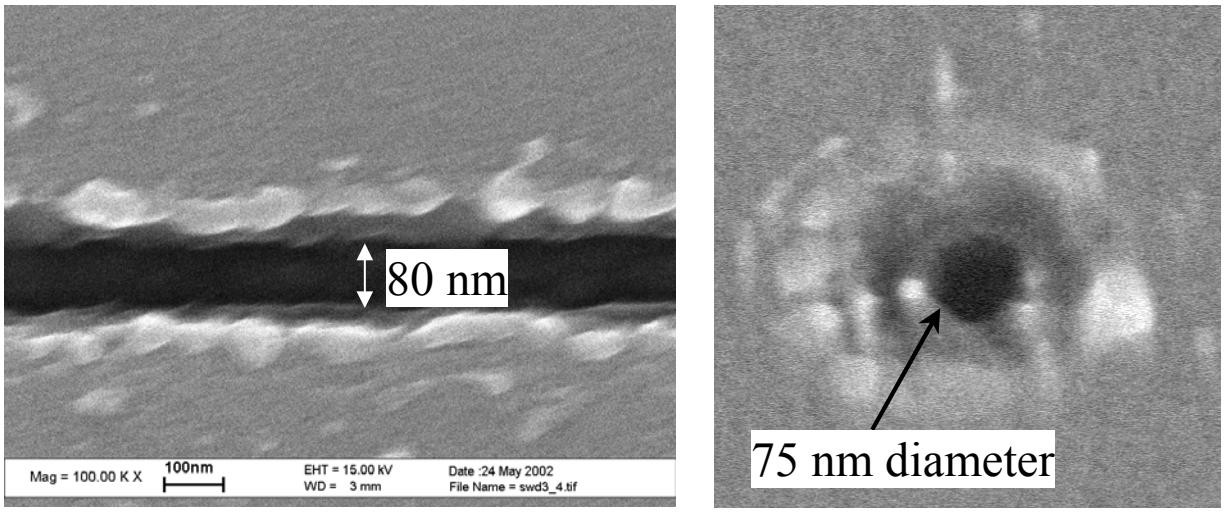

Figure 10: SEM micrographs of ablated line (a) and dot (b) which are substantially smaller than the approximately 150nm diameter of the focused laser spot.

AN ITERATIVE REPAIR STRATEGY: "NIBBLE MODE"

When a focused ion beam or a nanosecond pulsed laser is used to remove the absorber on a photomask, some degradation in the optical properties of the quartz substrate is inevitable. Typically, this forces the repair process to be limited to a single attempt. If the repair does not meet the requirements after the first attempt, additional attempts to trim the defect will result in cumulative degradation of the quartz substrate. This generally results in an optically unacceptable repair in leading edge masks due to excessive phase errors (quartz removal and river bedding) or transmission reduction (gallium stains). While in principal it should be possible to produce a "perfect" repair on the first attempt, the practical reality is that probability of an acceptable repair on the first attempt with a FIB tool is far below 100%. For the most complex, expensive masks, defects are sufficiently numerous that the overall probability of repairing EVERY defect to required specifications on the first attempt is unacceptably small. A new approach is needed.

Femtosecond laser ablation provides an alternative path. Since repeated ablations with the femtosecond laser beam do NOT cause cumulative damage to the quartz substrate, there is no need to produce a "perfect" repair on the first attempt. In fact, for the most demanding repairs we have found it advantageous to intentionally remove a defect in stages - essentially nibbling away at the defect in a series of repairs until the desired edge accuracy and optical transmission is obtained.

The following experiment demonstrates the outstanding edge placement precision that we have achieved with the MARS2 tool by iteratively trimming a feature. Figure 11 illustrates the experimental procedure.

Figure 11: (a) The gap between 2 Cr features is measured using the DUV image available in the repair tool. A thin slice of Cr is ablated (b) and the gap is remeasured. DUV images of the Cr pattern illustrating the process is shown in Figure 12. The process is repeated many times to obtain the data shown in Figure 13.

The width of a gap between Cr features was determined using the DUV image available in the MARS2 tool. A thin, programmed slice of Cr was then ablated from the edge of the feature, a new DUV image taken, and a new measurement of the gap obtained. The process of trimming a thin slice of Cr, and measuring the resulting change in gap width was repeated numerous times. The architecture of the MARS2 tool allows a minimum slice increment of approximately 23nm. Thus if the ablation process were perfectly reproducible, and the tool behaved perfectly, each successive slice should remove exactly 23 nm of additional Cr. Figure 12 shows actual DUV images from the MARS2 tool (a) before and (b) after the ablation of 7 individual slices of Cr. The gap between the Cr lines was determined by analyzing these images with a standard metrology software package.

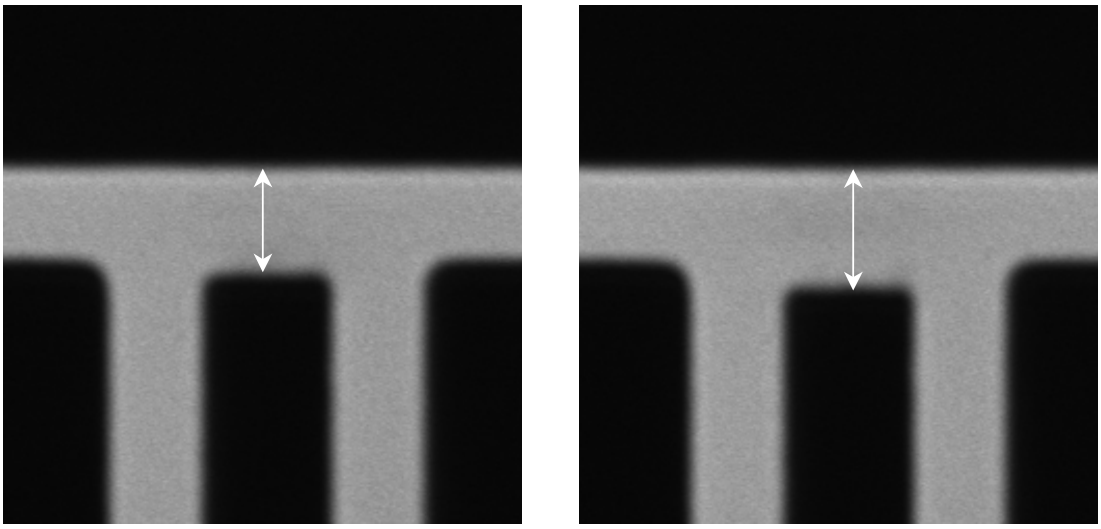

Figure 12: (a) DUV image of Cr lines before ablation. The arrow indicates the width of the gap between the lines. (b) DUV image after 7 slices of Cr were ablated; each slice removes approximately 23 nm of Cr.

The measured width of the gap as a function of the cumulative number of ablated Cr slices is shown in Figure 13(a). The measured width increases smoothly and monotonically with successive slices. A least squares linear fit to the data yields a slope of 22.77 +/- 0.12 nm per slice, precisely what is expected based on the tool architecture. The difference between the measured and the expected Cr gap as a function of the number of slices is shown in Figure 13(b). This graph illustrates the reproducibility, and hence precision of the ablation process and tool. The results indicate that a Cr line can be trimmed to an RMS precision of +/- 5.1nm. The maximum difference between the expected and actual position of the Cr edges (i.e. the gap width) was +/- 9nm. These results indicate that the tool and the ablation process combined are capable of achieving an edge placement accuracy with an RMS error of 5.1nm by iteratively trimming the defect.

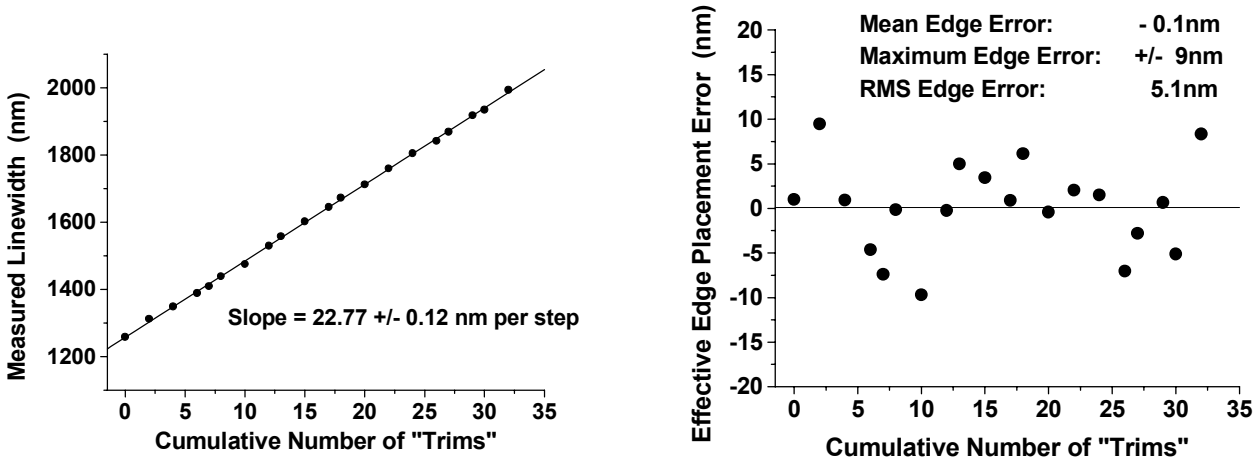

Figure 13: (a) Measured gap between Cr features as a function of the number of ablation slices. Each slice removes 22.77nm of Cr. (b) The difference between the measured and expected width of the gap for 20 successive trims of the Cr edge. The maximum error was +/- 9nm, and the RMS error was 5.1nm.

SUMMARY

We have developed an advanced tool for repairing opaque defects in photomasks. The tool images the mask in the DUV with 100nm resolution. A femtosecond laser beam is focused to a 150nm gaussian spot and scanned over the defect to remove it. Since the defect ablation process is non-thermal, masks can be repaired with minimal loss in optical transmission or damage to the quartz substrate. An ablation resolution of approximately 80nm was demonstrated and a procedure for iteratively repairing a defect with an RMS edge placement error of ~5nm was described. This tool is in routine manufacturing operation in the IBM mask house in Burlington, VT. Finally, the technology can be extended to achieve a substantial improvement in spatial resolution, through pellicle repair, and clear defect repair.

ACKNOWLEDGEMENTS

We would like to thank our colleagues and the management in the IBM Burlington mask house for supporting this work.

REFERENCES

1) A. Wagner, "Applications of Focused Ion Beams", Nucl. Instr. and Methods, 218, 355 (1983).

2) R. Hagiwara, A. Yasaka, O. Takaoka, T. Kozakai, S. Yabe, Y. Koyama, M. Muramatsu, T. Doi, K. Suzuki, M. Okabe, K. Aita, T. Adachi, S. Kubo, N. Yoshioka, H. Morimoto, Y. Morikawa, K. Iwase, N. Hayashi, "Advanced FIB Mask Repair Technology for ArF Lithography", SPIE 4409, 555 (2001).

3) L. Scipioni, D. Stewart, D. Ferranti, A. Saxonis,, "Performance of Multicusp Plasma Ion Source for Focused Ion Beam Applications", J. Vac. Sci. Technol. B18, 3194 (2000)

4) J. Morgan, T. Morrison, D. Ferranti, D. Stewart, "Progress for Characterization and Advanced Reticle Repair, Solid State Technol. 43, 195 (2000)

5) J. K. Tison and M. G. Cohen, "Lasers in Mask Repair", Solid State Technology, 113 (1987).

6) Yoshino, Y. Morishige, Y. Watanabe, S. Kyusho, Y. Ueda, A. Haneda, T. Ohmiya, M., "High accuracy laser mask repair system LM700A", SPIE 4186, 663 (2001).

7) P. Yan, Q. Qian, J. McCall, J. Langston, Y. Ger, J. Cho, B. Hainsey, "Effect of Laser Mask Repair Induced Residue and Quartz Damage in sub-half micron DUV Wafer Process", SPIE, 2621, 158 (1995).

8) J. D. Casey Jr., A. F. Doyle, D. K. Stewart, D. Ferranti, "Chemically Enhanced FIB Repair of Opaque Defects on Chrome Photomasks", SPIE 3096, 322 (1997).

9) A. Wagner and J.P. Levin, "Focused Ion Beam Repair of Lithographic Masks", Nucl. Instr. And Methods, B37/38, 224 (1989).

10) R. Haight, D. Hayden, P. Longo, T. Neary, and A.Wagner, SPIE 3546, 477 (1998).

11) R. Haight, D. Hayden, P. Longo, T. Neary, and A.Wagner, J. Vac. Sci. Technol. B17(6), 3137 (1999).

12) C. Korner, R. Mayerhofer, M. Hartmann, H.W. Bergmann, "Physical and Material Aspects in Using Visible Laser Pulses of Nanosecond Duration for Ablation", Appl. Phys. A., 63,123 (1996).

13) B. N. Chichkov, C. Momma, S. Nolte, F. Von Alvensleben, A. Tunnermann, “Femtosecond, Picosecond, and Nanosecond Laser Ablation of Solids”, Appl. Phys. A, 63, 109 (1996).

14) P. P. Pronko, S. K. Dutta, D. Du, R. K. Singh, “Thermophysical Effects in Laser Processing of Materials with Picosecond and Femtosecond Pulses”, J. Appl. Phys., 78, 6233 (1995).

15) M. Schmidt, P. Flanigan, D. Thibault, these proceedings